



**HAL**  
open science

**New isomeric states in  $^{152,154,156}\text{Nd}$  produced by  
spontaneous fission of  $^{252}\text{Cf}$**

C. Gautherin, M. Houry, W. Korten, Y. Le Coz, R. Lucas, X H. Phan, C.  
Theisen, C. Badimon, G. Barreau, T.P. Doan, et al.

► **To cite this version:**

C. Gautherin, M. Houry, W. Korten, Y. Le Coz, R. Lucas, et al.. New isomeric states in  $^{152,154,156}\text{Nd}$  produced by spontaneous fission of  $^{252}\text{Cf}$ . The European physical journal. A, Hadrons and Nuclei, 1998, 1, pp.391-397. in2p3-00003427

**HAL Id: in2p3-00003427**

**<https://in2p3.hal.science/in2p3-00003427v1>**

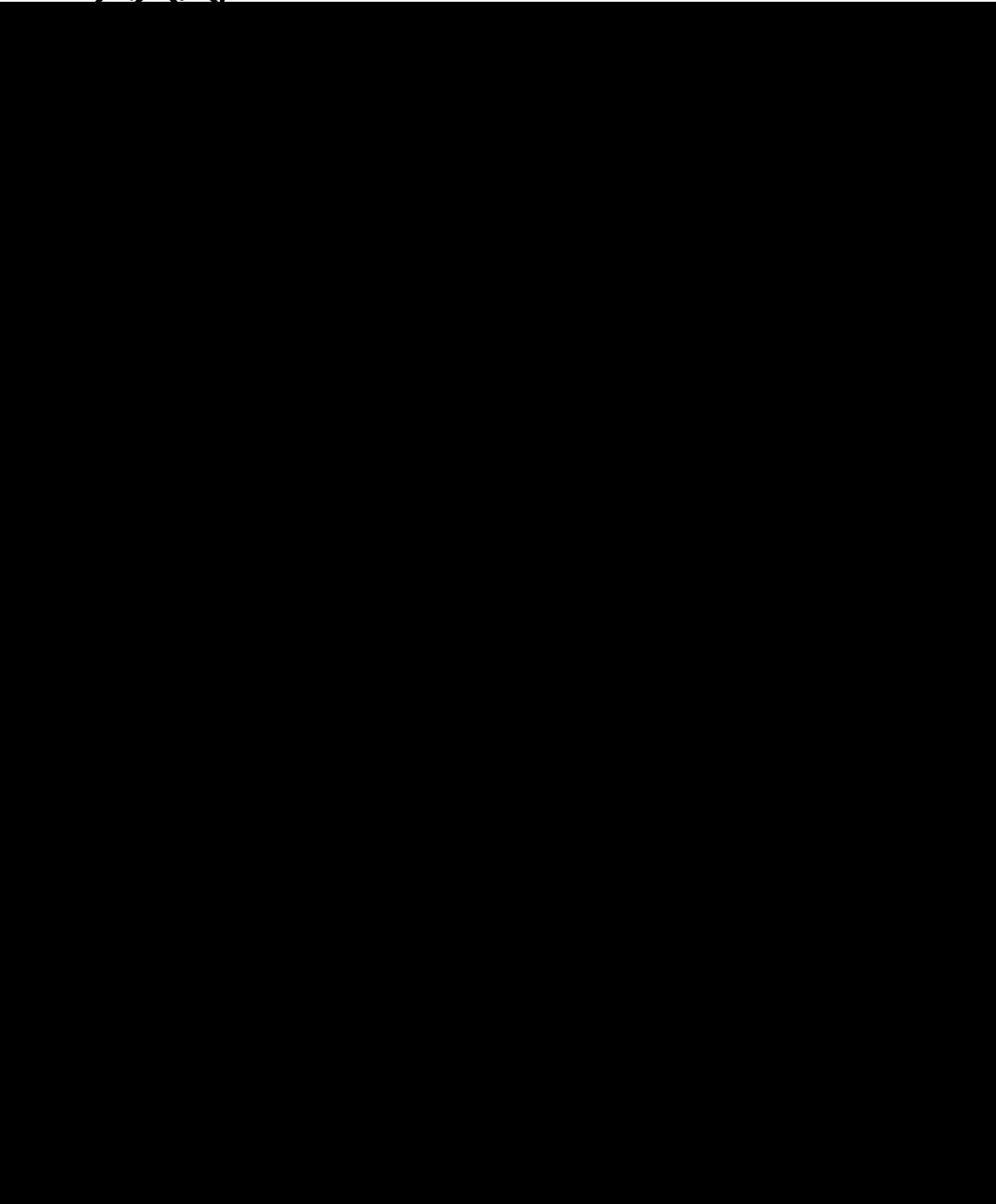
Submitted on 9 Dec 1998

**HAL** is a multi-disciplinary open access archive for the deposit and dissemination of scientific research documents, whether they are published or not. The documents may come from teaching and research institutions in France or abroad, or from public or private research centers.

L'archive ouverte pluridisciplinaire **HAL**, est destinée au dépôt et à la diffusion de documents scientifiques de niveau recherche, publiés ou non, émanant des établissements d'enseignement et de recherche français ou étrangers, des laboratoires publics ou privés.

22

○○○



To be published to European Physical  
Journal A

# New isomeric states in $^{152,154,156}\text{Nd}$ produced by spontaneous fission of $^{252}\text{Cf}$

C. Gautherin<sup>1</sup>, M. Houry<sup>1</sup>, W. Korten<sup>1</sup>, Y. Le Coz<sup>1</sup>, R. Lucas<sup>1</sup>, X.H. Phan<sup>1</sup>, Ch. Theisen<sup>1</sup>, Ch. Badimon<sup>2</sup>, G. Barreau<sup>2</sup>, T.P. Doan<sup>2</sup>, G. Pedemay<sup>2</sup>, G. Bélier<sup>3</sup>, M. Girod<sup>3</sup>, V. Méot<sup>3</sup>, S. Peru<sup>3</sup>, A. Astier<sup>4</sup>, L. Ducroux<sup>4</sup>, M. Meyer<sup>4</sup>, and N. Redon<sup>4</sup>

<sup>1</sup> CEA/Saclay, DSM/DAPNIA/SPhN, F-91191 Gif sur Yvette Cedex, France

<sup>2</sup> Centre d'Etudes Nucléaires Bordeaux-Gradignan Domaine du Haut Vigneau 33175 Gradignan, France

<sup>3</sup> Commissariat à l'Energie Atomique Bruyères-le-Châtel, DAM /SPN, BP12, F-91680 Bruyères-le-Châtel, France

<sup>4</sup> Institut de Physique Nucléaire Lyon, F-69622 Villeurbanne Cedex, France

Received : / Accepted:

**Abstract.** Isomeric states have been observed in fission-fragments produced by spontaneous fission of  $^{252}\text{Cf}$ . These states are found in neutron rich nuclei of different structure and deformations. About 50 isomeric nuclei have been observed using coincidences between  $\gamma$ -rays identified in EUROGAM II and fission fragments detected in photovoltaic cells (SAPhIR). Lifetimes in the range from 20 ns to  $2\mu\text{s}$  have been measured. Presented calculations based on HFB +D1S force on new measured isomeric states in the  $^{152,154,156}\text{Nd}$  show evidence for K-isomers.

**Key words:** 21.10, 21.60, 23.20, 84.60

## 1 Introduction

Extensive spectroscopic studies have been performed on spontaneous fission fragments of  $^{252}\text{Cf}$  (see for example [1, 2]). A renewal of interest for fission fragment spectroscopy occurred with the advent of large Ge detector arrays such as EUROGAM or GAMMA-SPHERE. Fission has been known since a long time to provide large numbers of rich neutron nuclei which are, for the most part, accessible in no other manner and which are released with various excitation energies, spins and deformations. They de-excite by neutron emission (within  $10^{-14}\text{s}$  after fission) and  $\gamma$ -transitions; these transitions end with the fragments reaching their ground states within about 1-2 microseconds after fission. These neutron-rich fragments then undergo  $\beta$  decay: the  $\beta$  decay process begins to have significant yield a few milliseconds after fission. The fission fragments are mainly found in three regions of the periodic table: the  $A=90-110$ ,  $Z=38-46$  region for which there is evidence of large deformations; the nuclei around the double magic  $^{132}\text{Sn}$  nucleus where single configurations coupled to the closed shells predominate; the region with  $A=140-160$ ,  $Z=52-64$  where there is a smooth transition from spherical to deformed nuclei.

Detailed experiments have been recently performed on the  $\gamma$  decay paths in excited fission fragments and thus have enhanced the possibilities to gain new insights in

nuclear structure (see for example [3, 4, 5]). However, in these new experiments, only prompt or short lived  $\gamma$ -rays have been measured. On the other hand, a large body of informations has been acquired for nuclei long-lived enough to be studied with on-line mass separator or radiochemical techniques (see for example [6]); in both methods, one is concerned with the so called fission products resulting from  $\beta$ -decay of the primary fission fragments.

The work presented in this paper deals with isomeric transitions occurring in the primary fission fragments within 1 microsecond after fission. A systematic study of delayed  $\gamma$  transitions occurring in the time range from a few ns up to 1 microsecond after the detection of the two complementary fission fragments has been undertaken. New isomeric states have been discovered. In Sect.2, the experimental set-up and methods are described. The experimental and theoretical results are shown in Sect.3 and 4 with a more precise study of isomers found in the Nd region, and the Sect.5 deals with the perspectives offered by the results.

## 2 The experiment

### 1. Experimental set-up.

The  $^{252}\text{Cf}$  source was deposited on a thin nickel backing, ( $110\mu\text{g}$  per  $\text{cm}^2$ ) and had an activity of about 1500 fissions/s. The aim of the performed experiment was to detect fission fragments produced in coincidence with the delayed  $\gamma$  rays emitted by the fragments. The two fragments were detected by two photovoltaic cells placed at 5 mm on both sides of the source to preserve the whole efficiency of EUROGAM II. The cells, we have used in this work, are commercially solar cells made of polycrystalline silicon with an active area of  $3\text{cm}^2$  and 500 microns thick. They are a good tool to detect fission fragments and their response is quite similar to more expensive surface barrier detectors [7]: their low cost as well as their low mass and simplicity of operation (no bias voltage required) are normally well suited for a combination with gamma-rays spectroscopy. The simple device we have used is part of the SAPhIR detector consisting of 48 solar cells devoted

to the detection of fission fragments. For further readings about photovoltaic cells, see also [9, 10].

The  $\gamma$  rays emitted by the fragments were detected by the EUROGAM II array [11, 12] at CRN Strasbourg (France), composed of 54 Compton-suppressed germanium detectors: 30 coaxial detectors at forward and backward angles and 24 clover [13] detectors around 90 degrees relative to the beam axis. The electronics used for the cells was VXI germanium card of EUROGAM, except that we have used external energy amplifiers more suitable than the ones designed for the germanium channels. The energy outputs were routed to the VXI ADC's. Events were recorded with the condition that the 2 cells fired in coincidence (start). Prompt and delayed  $\gamma$ -rays following fission (from 0 to  $1\mu$ s) were detected using the germanium detectors of EUROGAM II. Fragments striking the front face of the solar cells are stopped rapidly ( $10^{-12}$  s) giving rise to sharp delayed  $\gamma$  lines (no Doppler correction needed), the intensity of which is scanned up to  $1\mu$ s after fission.

## 2. Data analysis:

During the 10 days experiment we obtained for the delayed events  $6 \cdot 10^7$  Fr-Fr- $\gamma$  and  $5 \cdot 10^5$  Fr-Fr- $\gamma$ - $\gamma$  coincidences. The pulse height spectrum measured with the 2 cells is shown in 0.1a.

The masses of the fragment have been extracted from their energies. From each event, the energy to mass conversion was performed by an iterative process which takes into account both the mass dependent energy calibration of Schmitt et al [14] and the neutron emission by the fragments: The average neutron multiplicities per fragment mass  $\bar{\nu}(m)$  have been taken from the recent measured values of Düring et al [16]. The use of the  $\bar{\nu}(m)$  measurements of Signarbieux and Budtz-Jorgensen respectively, give some differences in the relevant post-neutron mass distribution without affecting its general trend. [17, 18]. The global post-neutron mass distribution deduced from this analysis (see Fig. 1.b.) exhibits the 2 well known humps centered around  $A=106$  and  $A=142$  (masses after neutron evaporation). We then obtain for each event the 2 fission fragment masses and kinetic energies, the  $\gamma$ -rays energies and their emission time after fission. Events were sorted by EURO13 software [19] and analysed with the Radware package [20]. At the end, one obtains the energy, half life and intensity of each  $\gamma$ -ray as well as an estimation of the mass of the fission fragments.

The time spectrum between fragments and prompt  $\gamma$ -rays has a resolution of about 20 ns. Using this time spectrum, one can easily separate the prompt and the delayed  $\gamma$ -rays and measure the half live of the identified isomeric levels (Fig. 2). In  $^{252}\text{Cf}$  7% of the fission fragments  $\gamma$ -rays were found to be isomeric in the range of half-lives less than  $3\mu$ s.

## 3 Results on isomeric $\gamma$ -rays

The fission fragment  $\gamma$ -ray trigger has been found to be much clearer than the  $\gamma$ - $\gamma$  trigger alone as the Fragment-

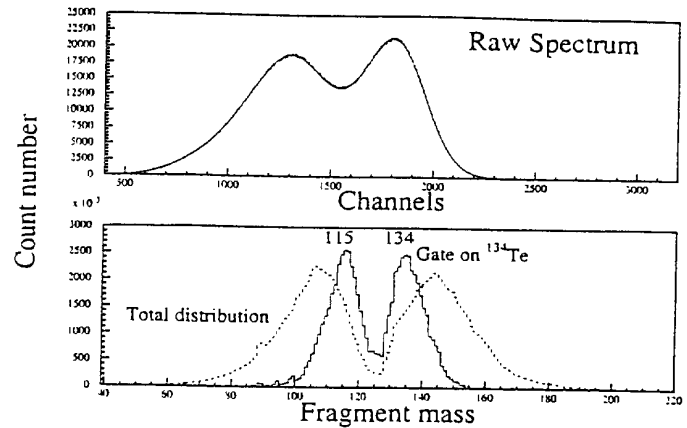


Fig. 1. a Pulse height spectrum of  $^{252}\text{Cf}$  spontaneous fission measured with photovoltaic cells. b dashed line: Total post neutron evaporation mass distribution of  $^{252}\text{Cf}$  fission fragments, continuous line: mass distribution obtained with a gate on the 1279 keV level of  $^{134}\text{Te}$ .

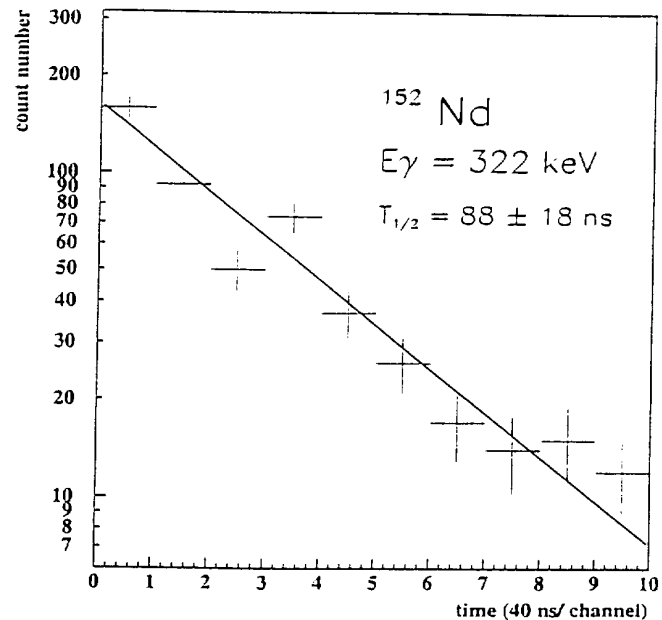


Fig. 2. Example of decay of the intensity of  $\gamma$ -ray as a function of time allowing to determine the half life of the considered isomer, here  $^{152}\text{Nd}$ .

Fragment coincidences could not be triggered on background radiation as easily as the  $\gamma$ - $\gamma$  trigger. More than 300 delayed  $\gamma$ -rays have been identified.

Isomeric levels belonging to about 60 neutron rich nuclei have been identified, where only one part was already known. On Fig.3 the different nuclei where we found isomeric states are presented. Very neutron rich nuclei are populated (richer than in induced fission as, in this case,

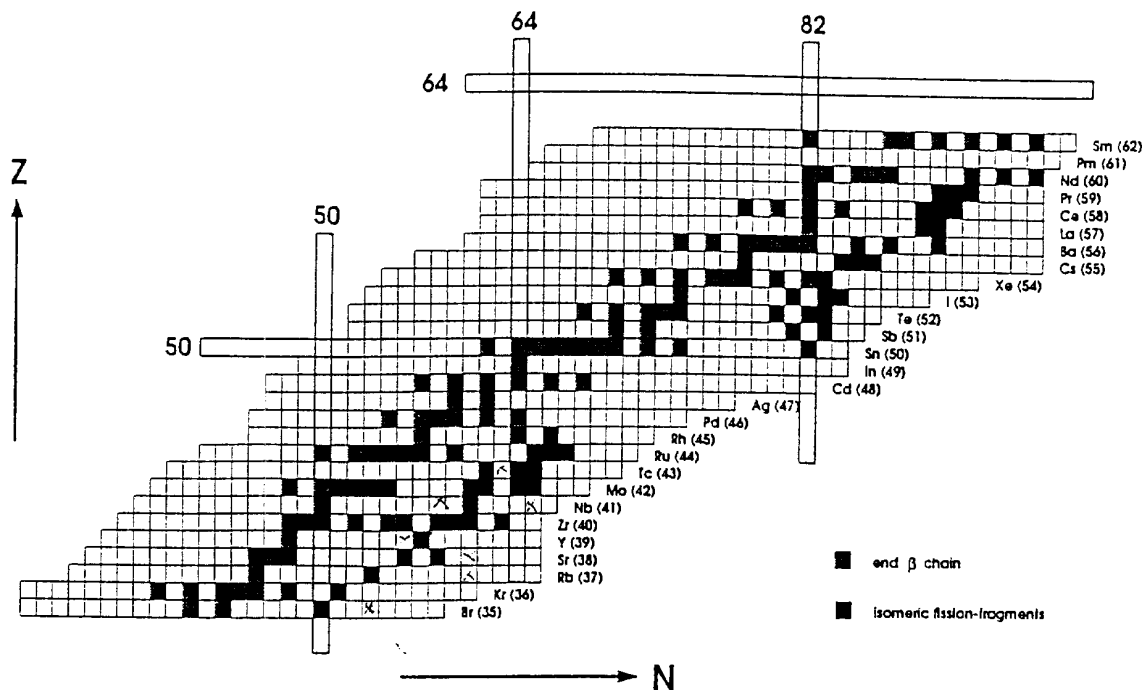


Fig. 3. In this Z-N chart of nuclei  $\beta$  stable nuclei are colored in grey. In black are shown nuclei where isomeric states have been identified in the spontaneous fission of  $^{252}\text{Cf}$ . (this work)

the excitation energy is higher and allows neutron evaporation) corresponding to 13 odd-odd, 18 even-even, 15 even-odd and 13 odd-even nuclei.

In order to show the selectivity obtained in this kind of experiment, we show on Fig. 4a the  $\gamma$  spectrum obtained in coincidence with the fission fragments. In Fig. 4b only the delayed events are taken into account and on Fig. 4c a gate on the 1436 keV  $\gamma$ -ray is required. The 1436 keV  $\gamma$ -ray belongs to the  $^{138}\text{Ba}$  as well as to the  $^{152}\text{Nd}$  nuclei. Gating on it, we obtain the  $4^+ \rightarrow 2^+$  463 keV and the  $6^+ \rightarrow 4^+$  192 keV  $\gamma$ -rays of  $^{138}\text{Ba}$  nucleus as well as the  $2^+ \rightarrow 0^+$  72 keV, the  $4^+ \rightarrow 2^+$  164 keV, the  $6^+ \rightarrow 4^+$  247 keV and the  $8^+ \rightarrow 6^+$  322 keV  $\gamma$ -rays of  $^{152}\text{Nd}$ . It has to be noted that this last spectrum was obtained without any background subtraction.

It should be emphasized that, due to the choice of the trigger (coincidences between the 2 fission fragments), the  $\gamma$  rays from both fragments are observed in coincidences with those fission fragments, thus it is difficult to attribute unknown  $\gamma$ -rays to light or heavy partner. When gating on one particular  $\gamma$ -ray, one obtains a mass distribution with 2 humps (for example, gating on the 1279 keV  $\gamma$ -ray of  $^{134}\text{Te}$ , the mass distribution is peaked at  $A=115$  and 134 with a mass resolution (FWHM) of about 10% for each hump (Fig. 1b)). Gamma-gamma coincidences have been used to build-up the level scheme for several nuclei but a few delayed gamma transitions have not yet been attributed. In the following, we present our study of isomeric states in rare earth isotopes. A review of isomeric states in other mass regions will be published [21].

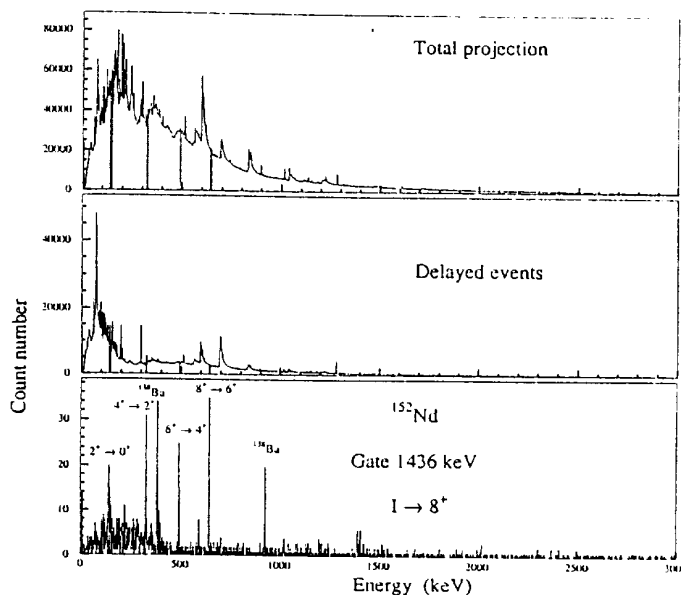


Fig. 4. Example of  $\gamma$  delayed and  $\gamma$ -gated selectivity. a Total projection of the  $\gamma$  spectrum; b same as a but with only the delayed events; c gate on the 1436 keV  $\gamma$ -ray. We clearly see in coincidence with the 1436 keV the different  $\gamma$ -rays characteristic of  $^{138}\text{Ba}$  and  $^{152}\text{Nd}$  nuclei.

### 3.1 Study of neodymium isomers.

#### 3.1.1 $^{152}\text{Nd}$

The low lying levels in  $^{152}\text{Nd}$  are known from studies of prompt  $\gamma$ -rays in spontaneous fission of  $^{252}\text{Cf}$  [1, 22] and

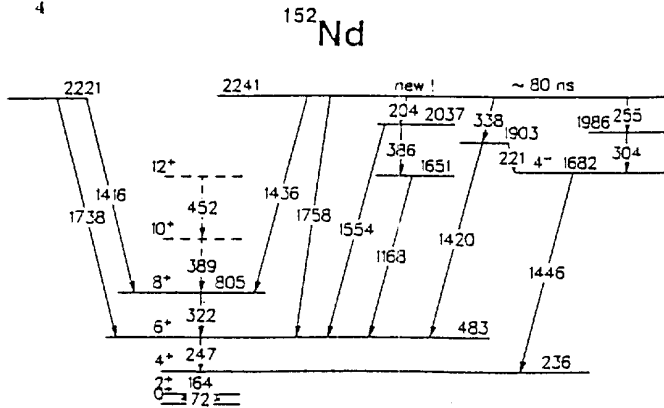


Fig. 5. Partial level scheme of  $^{152}\text{Nd}$  (prompt transitions are marked with dashed lines).

from the  $\beta$ -decay of  $^{152}\text{Pr}$  [23, 24]. This nucleus is the first neodymium isotope showing a clear level sequence of axially deformed nuclei, the evolution of  $E(4_1^+)/E(2_1^+)$  energy ratios of 2.49 for  $^{148}\text{Nd}$ , 293 for  $^{150}\text{Nd}$  and 3.27 for  $^{152}\text{Nd}$  indicating furthermore a transitional region from spherical to deformed nuclei. Before this work, the only measured delayed levels were the lower part of the rotational band starting from  $6^+ \rightarrow 4^+$  as well as the  $4^-$  state at 1682 keV excitation energy depopulating via a 1446 keV towards the  $4^+$  state [24]. This decay transition was interpreted to be a member of a  $K=2$  octupole band (1683.5 keV in [23]).

A lot of delayed transitions, all with the same half life ( $80 \pm 15$  ns), have been identified and are shown on Fig. 5. All these transitions depopulate the level at 2241 keV. The 1416 keV and 1738 keV  $\gamma$ -rays coming from a level at 2221 keV are also probably issued from the level at 2241 keV but the 20 keV connecting these 2 levels are below our detection threshold. This 2241 keV isomer is directly connected to the rotational band with two transitions of 1436 keV ( $I \rightarrow 8^+$ ) and 1758 keV ( $I \rightarrow 6^+$ ). The building of the level scheme was complexified by the presence of the 204 keV  $\gamma$ -ray which belongs to  $^{152}\text{Nd}$  as well as to one of the companion  $^{91}\text{Sr}$ . The use of  $\gamma$ - $\gamma$  coincidences allowed to disentangle this ambiguity.

### 3.1.2 $^{154,156}\text{Nd}$

The yrast rotational bands in  $^{154}\text{Nd}$  and  $^{156}\text{Nd}$  are characteristic of well deformed collective quadrupole deformations with an  $E_4/E_2 = 3.26$  and 3.31 (quite a perfect rotor), the energies of levels in the yrast bands having the same spin decrease smoothly with increasing neutron number. This indicate increasing deformations up to high spin states. For  $^{156}\text{Nd}$  an isomer populating the  $6^+$  and the  $4^+$  states of the rotational band is found with a half-life of 135 ns (see Fig. 6), the two delayed transitions having equivalent intensities. For  $^{154}\text{Nd}$  we see delayed transitions populating the  $6^+$  (half life greater than  $1\mu\text{s}$ ) and the  $4^+$  states but the transition populating the  $4^+$  level has a very low intensity (the intensity of the delayed transition populating the  $6^+$  level is seven times

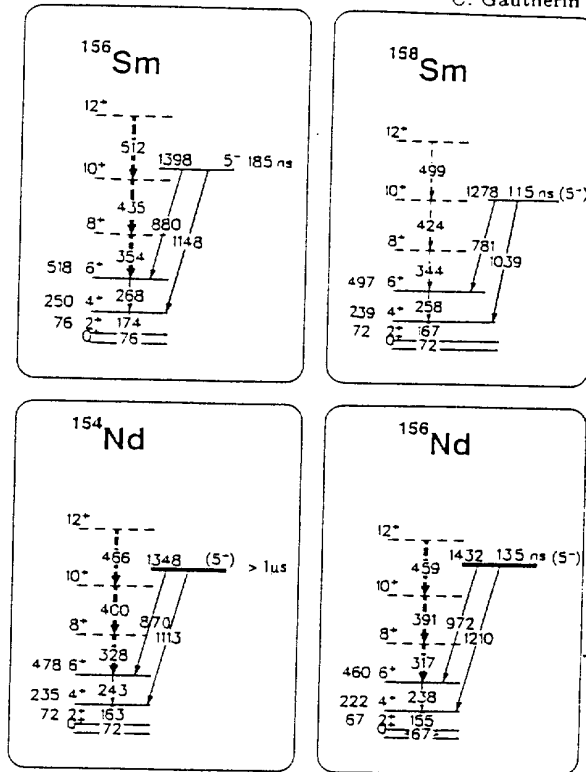


Fig. 6. Partial level schemes of  $^{156,158}\text{Sm}$  and  $^{154,156}\text{Nd}$  (prompt transitions are marked with dashed lines).

more intense than the delayed transition populating the  $4^+$  level).

We can compare these results with those obtained for the isotones  $^{156}\text{Sm}$  and  $^{158}\text{Sm}$ , respectively. The level at 1398 keV in  $^{156}\text{Sm}$  with lifetime of 185 ns was observed in earlier work [24]; spin and parity for this level are identified as  $5^-$  which was interpreted in terms of  $(\nu 5/2 [642] \otimes \nu 5/2 [523]) 5^-$  neutron states (see Fig. 6). We confirm the two transitions  $5^- \rightarrow 6^+$  and  $5^- \rightarrow 4^+$ . Another level at 113 keV, which feed the level at 1398 keV and has a 4.5 ns half life, was not seen in this work due to the too short lifetime. These levels probably belong to a collective band with a spin/parity assignment of  $5^-$  for the band head. We found the same kind of scheme for  $^{158}\text{Sm}$  as Zhu et al [22] where they assigned a spin and a parity of  $5^-$  for the level at 1279 keV; for this isomeric level the half life has been measured to be 115 ns. From theoretical calculations this band head has probably the 2QP configuration similar to the band in  $^{156}\text{Sm}$ . Evidences found for isomeric transitions feeding the low energy rotational states in deformed even-even rare earth Nd isotopes are similar to those obtained in  $^{156}\text{Sm}$  and  $^{158}\text{Sm}$ . The similar behaviour of the isomers in  $^{156}\text{Nd}$  compared to  $^{156}\text{Sm}$  and  $^{158}\text{Sm}$  suggests that the isomeric state in  $^{156}\text{Nd}$  can be interpreted as being low lying QP states whose decay into the ground state band is  $K$  forbidden. The relative intensities of the isomeric  $\gamma$ -rays are quite similar. The ratio of intensities of isomeric  $\gamma$ -rays populating the  $6^+$  and the  $4^+$  of the rotational bands of  $^{156}\text{Nd}$ ,  $^{156}\text{Sm}$  and  $^{158}\text{Sm}$  are respectively of 0.99, 0.87 and 0.58.

#### 4 Theoretical considerations

The interpretation of these experimental data is presented in the framework of the Hartree-Fock-Bogoliubov (HFB) theory, in which the finite range and density dependent force DIS of Gogny is used thoroughly. The isomeric states are treated as two proton or neutron quasiparticle (2QP) excitations built on the ground state (GS). Prior to this study, it is necessary to determine the structure of the GS level. For this purpose, we have performed constrained HFB calculations intended to obtain potential energy surfaces (PESs) of each nucleus [26]. These surfaces are built from the minimization :

$$\delta \langle \Phi_q | \hat{H} - \lambda_0 \hat{Q}_{20} - \lambda_2 \hat{Q}_{22} | \Phi_q \rangle = 0. \quad (1)$$

where  $\Phi_q$  is the quasiparticle (QP) vacuum,  $\hat{H}$  the many-body nuclear Hamiltonian,  $\hat{Q}_{20}$  and  $\hat{Q}_{22}$  external field operators which generate axial and triaxial quadrupole deformations, respectively. In the actual calculations, the proton and neutron numbers are also constrained so that

$$\langle \Phi_q | \hat{Z} \text{ (or } \hat{N}) | \Phi_q \rangle = Z \text{ (or } N).$$

Once the constrained HFB equations are solved for  $\langle \hat{Q}_{20} \rangle = q_{20}$  and  $\langle \hat{Q}_{22} \rangle = q_{22}$ , the potential energy surfaces are defined as

$$V(q) = \langle \Phi_q | \hat{H} | \Phi_q \rangle,$$

where the notation  $q = (q_{20}, q_{22})$  is used. Since  $q_{20}$  and  $q_{22}$  are directly related to the Bohr coordinates  $\beta$  and  $\gamma$ , the potential energy surface (1) may also be expressed as  $V(\beta, \gamma)$ .

The PES  $V(\beta, \gamma)$  are shown in Fig.7 for  $^{152,154,156}\text{Nd}$  isotopes. As can be seen, these surfaces display deep minima at large prolate deformation (i.e.  $\beta_{min} \simeq 0.35$ ). Going a step further, we have also performed configuration mixing calculations in the GCM+GOA framework [27]. The excitation energies of the GS rotational bands predicted with this method are in good agreement with experimental data (see Fig 8). Furthermore, we have found that the GS mean dynamic deformation  $\sqrt{\langle \beta^2 \rangle}$  is nearly identical to  $\beta_{min}$ . With this latter result, we feel it justified to take as QP vacuum the HFB wave function which minimizes the potential energy. This implies that in first approximation, we can neglect the particle vibration coupling.

The 2QP states are defined :

$$|\tilde{\Phi}_{bb'} \rangle = \eta_b^\dagger \eta_{b'}^\dagger |\Phi \rangle$$

where  $|\Phi \rangle$  is a HFB vacuum (see eq.1), and  $b$  and  $b'$  are labels for the quantum numbers of the blocked quasiparticles.

Since axial symmetry is imposed,  $b$  represents the following set of quantum numbers : the projection  $\Omega$  of the angular momentum on the  $z$  axis, the parity  $\pi$ , and the signature  $\alpha$ . To obtain the first 2QP states, it is natural to choose the blocked states among states near the Fermi level of the HFB vacuum state of each nucleus. Blocking QP states spontaneously breaks time reversal

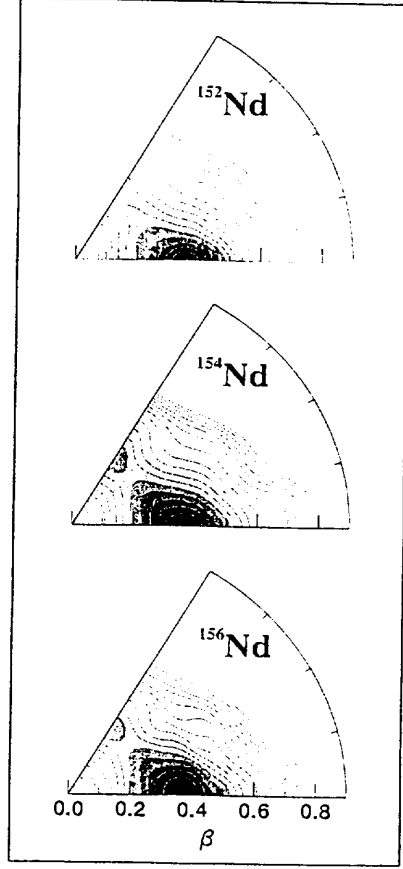


Fig. 7. PES  $V(\beta, \gamma)$  for  $^{152,154,156}\text{Nd}$  isotopes.

symmetry. Therefore, the degeneracy in energy between 2QP states with signatures  $\alpha = \pm 1$  is raised.

We have performed such calculations for the first neutron and proton 2QP states in the  $^{152,154,156}\text{Nd}$  and  $^{156,158}\text{Sm}$  nuclei. In Fig.8 are shown the excitation energies of the predicted 2QP states.

For each nucleus, the first 2QP signature partner states are neutron excitations. The proton 2QP states are close to the neutron 2QP states in the Samarium isotopes. In contrast, the proton 2QP states are lying at higher excitation energies in the Neodymium isotopes. From the comparison between these predictions and the experimental levels, we can make the following statements :

i) For  $^{158}\text{Sm}$ , the spin and parity  $I^\pi = 5^-$  assigned to the experimental level are consistent with the lowest predicted proton or neutron 2QP states ( $\pi 5/2[532] \otimes \pi 5/2[413]$ ) or ( $\nu 5/2[642] \otimes \nu 5/2[523]$ ).

ii) For  $^{156}\text{Sm}$ , the experimental  $5^-$  level is interpreted as the lowest proton 2QP state ( $\pi 5/2[532] \otimes \pi 5/2[413]$ ).

iii) For  $^{156}\text{Nd}$ , the experimental level for which no spin and parity are given might be the predicted  $5^-$  neutron 2QP state ( $\nu 5/2[642] \otimes \nu 5/2[523]$ ).



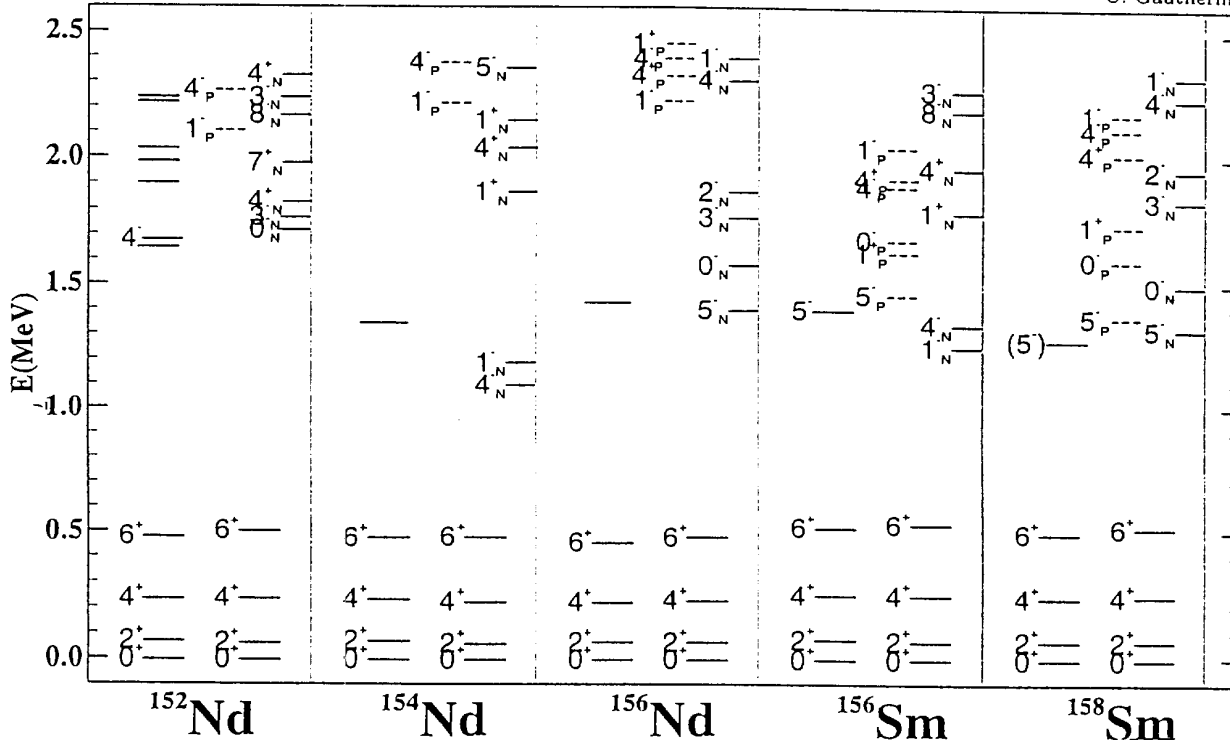


Fig. 8. First neutron and proton 2QP states in the  $^{152,154,156}\text{Nd}$  and  $^{156,158}\text{Sm}$  nuclei. The experimental (left part) and HFB ground state rotational bands are also shown.

iv) For  $^{154}\text{Nd}$ , the spin and parity  $I^\pi = 4^-$  or  $1^-$  ( $\nu$   $5/2[642] \otimes \nu$   $3/2[521]$ ) of the first neutron 2QP states are tentatively assigned to the experimental isomeric level. This attribution raises problems because this level decays to the  $6^+$  level of the GS band but not to the  $4^+$  at least with a measurable intensity. It seems that the only possible spin/parity assignment for this isomeric level would be  $6^-$ . However, the calculated first  $6^-$  2QP states are very high in energy ( $\approx 5$  MeV). Such a spin can also be obtained from 4QP states but they are located at about the same energy. A very conjectural possibility could be the collective nature  $K=6$  for this state.

v) For  $^{152}\text{Nd}$ , seven experimental levels are located in the energy range between 1.6 MeV and 2.3 MeV with unspecified spins and parities (except for a  $4^-$  state). We are unable to assign unambiguously spin and parity to these levels, but notice that the observed and predicted level densities in this energy range are very similar.

## 5 Conclusion and perspectives

We have measured isomeric states of half lives from 30 ns to  $2\mu\text{s}$  in more than 50 fission fragments of  $^{252}\text{Cf}$  spontaneous fission. Their intensities imply that about 10% of the deexcitation proceeds through the isomer. Some new isomers, identified in the rare earth region, show a behaviour which, according to HFB calculations, should correspond to K isomers. Angular distributions are still needed to assign spins and parities to the first isomeric states in rare earth region. At the opposite end of the deformed rare earth region a  $J^\pi K=3^+$  isomer is observed

in three  $N=106$  even  $Z$  nuclei going from W to Pt (half live of about 1 ms) [25]. These isomers feed the  $8^+$  member of the ground state band by a highly hindered E1 transition which accounts for 20-30% of the total population of the ground state band  $8^+$  level for  $^{182}\text{Os}$  and  $^{184}\text{Pt}$ , respectively. Such behaviour in the analogous fission fragment deexcitation process should not be completely unexpected, and the isomers in  $^{154,156}\text{Nd}$  could thus be interpreted as being low lying QP states whose decay into the ground state band is K forbidden. Moreover, spontaneous fission gives fragments in a particular zone of neutron rich nuclei. The possibility to obtain the kinetic energy distribution for each fragment is one of the advantage of having fission fragment detectors. The  $\gamma$ -rays intensities could be measured in coincidence with varying kinetic energy and fission fragment mass regions allowing to study the evolution of fragment yield as a function of excitation energy: this could bring new insights on the mechanism of angular momentum sharing between the fission fragments as well as on the dynamics of fission.

It will also be possible to cover more extended zones by using fission induced by reactions between different targets and heavy ion beams. So, we can say that study of isomers in fission fragments is a promising way to increase our knowledge of neutron rich nuclei.

*Acknowledgement.* We wish to thank the whole Eurogam staff of CRN Strasbourg. We are especially indebted to D. Curien, J. Devin, G. Duchêne, D. Prévost and C. Ring for their help during the experiment. Moreover we would like to thank L. Plateau and

D. Durand for their contribution in the ancillary set-up.  
Support for this work was provided by CEE (contract CHRX-CT  
930367).

This article was processed by the author using the  $\LaTeX$  style file  
*pljour2* from Springer-Verlag.

## References

1. R.G. Clark, L.E. Glendenin, W.L. Talbert Jr: Proc. Symp. Phys. Chem. Fission, 3rd, Rochester, N.Y. (1973), IAEA, Vienna. Vol.2, 221(1974)
2. W. John, F.W. Guy, J.J. Wesolowski: Phys. Rev. C2, 1451 (1970)
3. J. Durell: Conference on Physics from large detector arrays, Berkeley LBL 35687 Vol 1 (1994) 107
4. I. Ahmad and W.R. Phillips: Rep. Prog. Phys. 58 (1995) 1415
5. J.H. Hamilton, A.A. Ramayya, S.J. Zhu, G.M. Ter-Akopian, Y.Ts. Oganessian, J.D. Cole, J.O. Rasmussen, M.A. Stoyer: Prog.Part. Nucl. Phys., Vol 35 (1995) 635
6. D.C. Hoffmann, M.R. Lane:LBL 37467 (1995); Nucl. Physics A502 (1989) 21
7. G. Siegert Nucl. Instr. Meth. 164 (1979) 437 (1982) p2018.
8. Ch. Theisen, C. Gautherin, M. Houry, W. Korten, Y. Le Coz, R. Lucas, G. Barreau, Ch. Badimon, T. P. Doan, V. Méot, G. Bélier: Rapport CEA DAPNIA/SPhN 97-20 (1997)
9. N.N. Ajitanand, R.P. Anand, S.R.S. Murthy, K.N. Iyengar: NIM A300 354(1991)
10. E. Liatard, S. Akrouf, J.F. Bruandet, A. Fontenille, F. Glasser, P. Stassi, Tsan Ung Chan: NIM A267 231 (1988)
11. P.J. Nolan: Nucl. Phys. A520 657 (1990)
12. F.A. Beck: Prog. Part. Nucl. Phys. 28 443 (1992)
13. P.M. Jones, L. Wei, F.A. Beck, P.A. Butler, T. Byrski, G. Duchêne, G. de France, F. Hannachi, G.D. Jones, B. Kharraja: NIM A362 556(1995)
14. H.W. Schmitt, W.E. Kiker, C.W. Williams: Phys. Rev. 137 (1965) B837
15. G. Mamane, E. Cheifetz, E. Dafni, A. Zemel: Nucl. Phys. A454 (1986) 213
16. J. Düring, M. Adler, H. Märten, A. Ruben, B. Cramer, U. Jahnke: Proceedings of the International Workshop High resolution spectroscopy of fission fragments Dresden (1993) p104
17. C. Budtz-Jorgensen and H.H. Knitter: Nucl. Phys. A490,307 (1988)
18. C. Signarbieux, R. Babinet, H. Nifenecker and J. Poitou: Proc. Symp. Phys. Chem. Fission, 3rd, Rochester, N.Y. (1973), IAEA, Vienna, Vol.2, 117(1974)
19. Ch Theisen: unpublished
20. D. Radford: Nucl. Instr. and Meth. A361 (1995) 297, and Nucl. Instr. and Meth. A361 (1995) 306
21. C. Gautherin: Thesis (1997)
22. S.J. Zhu, J. H. Hamilton, A. V. Ramayya, B R S Bhabu, Q.H. Lu, W. C. Ma, T. N. Ginter, M. G. Wang, J. Kormicki, J. K. Deng, D. Shi, J. D. Cole, R. Aryaeinejad, J. Rasmussen, M. A. Stoyer, S. Y. Chu, K. E. Gregorich, M. F. Mohar, S. Prussin, G. M. Ter-Akopian, Yu Ts Oganessian, N. R. Johnson, I.Y. Lee, F. K. McGowan: J. Phys. G21 (1995) L57, L75
23. T. Karlewski: Z. Phys. A330, 55 (1988)
24. M. Hellström, B. Fogelberg, H. Mach, D. Jerrestam, L. Spanier: Phys. Rev C 41, 2325 (1990), Phys. Rev. C 43, 1462 (1991)
25. J. Burde, R.M. Diamond and F.S. Stephens: Nucl. Phys. A55 (1966) 481
26. J. Dechargé and D. Gogny: Phys. Rev. C21, 1568 (1980); M. Girod and B. Grammaticos: Phys. Rev. C27, 2317 (1983); J. F. Berger, M. Girod, and D. Gogny: Nucl. Phys. A428, 23c (1984); *ibid.* A502, 85c (1989); *ibid.* Comp. Phys. Comm. 63, 365 (1991).
27. K. Kumar and M. Baranger: Nucl. Phys. A110, 529(1968); K. Kumar. Nucl. Phys. A231, 189 (1974).

